Journal of Biomolecular NMR, **13:** 3–10, 1999.
KLUWER/ESCOM

Improved ^{1}HN-detected triple resonance TROSY-based experiments

Daiwen Yang & Lewis E. Kay
Protein Engineering Network Centers of Excellence and Departments of Molecular and Medical Genetics, Biochemistry and Chemistry, University of Toronto, Toronto, ON, Canada M5S 1A8

Received 17 July 1998; Accepted 12 August 1998

Key words: coherence transfer selection by gradients, triple resonance NMR, TROSY

Abstract

A pulse scheme resulting in improved sensitivity in TROSY-based ^{1}HN-detected triple resonance experiments is presented. The approach minimizes relaxation losses which occur during the transfer of transverse magnetization from ^{15}N to ^{1}HN immediately prior to detection. The utility of the method is demonstrated on a complex of methyl protonated, highly deuterated maltose binding protein (MBP, 370 residues) and β-cyclodextrin. Sensitivity gains relative to previous TROSY schemes of approximately 10 and 20% are noted in HNCO spectra of MBP recorded at 25 and 5 °C, respectively, corresponding to molecular correlation times of 23 and 46 ns.

Introduction

A major limitation in the application of NMR methodology to macromolecular studies remains the rapid decay of signal as a function of increasing molecular size. To this end the use of ^{2}H labeling (Kay and Gardner, 1997; Venters et al., 1996) in concert with heteronuclear, multidimensional NMR experiments (Bax, 1994) has significantly increased the scope of systems that can currently be studied. Solution structures of proteins or protein complexes in the 30 kDa molecular weight range are beginning to emerge (Garrett et al., 1997; Yu et al., 1997) and backbone assignments of molecules in the 40–60 kDa regime have been published (Farmer et al., 1996; Shan et al., 1996). More recently Pervushin and coworkers have reported that significant improvements in the sensitivity of important classes of experiments can be achieved by relying on the cancellation of contributions to relaxation from dipole-dipole and chemical shift anisotropy (CSA) relaxation mechanisms (Pervushin et al., 1997, 1998a). Specifically, in the case of ^{15}N-^{1}HN correlation based experiments recorded on macromolecules at high magnetic fields, this cross-correlation effect leads to very different intensities for each of the four multiplet components of a given amide correlation. Pulse sequences which are designed to ensure that exchange between multiplet components is minimized and which select the slowest relaxing component give rise to spectacular improvements in both resolution and sensitivity (Pervushin et al., 1997, 1998a; Wüthrich, 1998). In this report we demonstrate that still further improvements in sensitivity are possible in ^{1}HN detected TROSY-based triple resonance experiments by minimizing relaxation losses that occur during the transfer of magnetization from ^{15}N to ^{1}HN prior to detection.

Materials and methods

Triple-resonance TROSY-based pulse schemes were evaluated with HNCO sequences (Kay et al., 1990) (see Figure 2 and below) by recording 2D ^{15}N-^{1}HN (F_2, F_3) spectra on a sample of a 1.4 mM Val, Leu, Ile ($C^{\delta 1}$ only)-methyl protonated, highly deuterated maltose binding protein (MBP), 2 mM β-cyclodextrin, 20 mM sodium phosphate buffer pH 7.2, 3 mM NaN_3, 100 mM EDTA, 0.1 mg/mL Pefabloc, 1 μg/μL pepstatin and 10% D_2O (Gardner and Kay, 1997; Gardner et al., 1998). All NMR experiments were performed on a Varian Inova 600 MHz spectrometer at 25 or 5 °C. 2D data sets with 39 (^{15}N) and 576 (HN) complex points were acquired (acquisition times of 24.4

and 64 ms in the ^{15}N and ^{1}HN dimensions, respectively); 160 transients/FID and a repetition delay of 1.6 s was used to give a total measuring time of 5.5 hours/spectrum. Spectra were processed with NMR-Pipe (Delaglio et al., 1995) using sinebell-squared window functions shifted by 90° and 80° in the ^{15}N and ^{1}HN dimensions, respectively, and the ^{15}N dimension was doubled by mirror image linear prediction (Zhu and Bax, 1990) and extended to 512 points by zero filling prior to Fourier transformation while the ^{1}HN dimension was doubled by zero filling. Data analysis was performed with PIPP/CAPP (Garrett et al., 1991). The relative signal-to-noise (S/N) of spectra acquired with sequences (i) and (j) was calculated according to the relation

$$(1/N)\Sigma_k(S_{ik}/N_i)/(S_{jk}/N_j) \quad (1)$$

where S_{ik} is the height of peak k in experiment i, N_i is the noise floor level in experiment i, and N is the total number of peaks compared. S/N values in the experiments were quantitated on the basis of 83 well resolved crosspeaks in 2D spectra. Three-dimensional HNCO spectra of MBP were recorded with the sequences of Figures 2a and 2b at 5 °C and 270 peaks quantitated. Data matrices consisting of (22,36,576) complex points in (t_1,t_2,t_3) corresponding to acquisition times of (14.7 ms, 22.5 ms, 64 ms) in (F_1,F_2,F_3) were recorded with 16 transients/FID and a repetition delay of 1.6 s. The processing parameters for the ^{15}N and ^{1}HN dimensions of the 3D data sets were the same as those used in the 2D spectra; in the ^{13}C′ dimension a 90° shifted cosinebell window was employed. In the cases where both 2D and 3D spectra were recorded identical relative S/N values of crosspeaks (see Equation 1) were obtained from 2D and 3D data sets.

Results and discussion

The basic concept behind the TROSY-approach has been described in detail previously (Pervushin et al., 1997) and improvements in the original scheme were presented recently by K. Wüthrich at a meeting in Oxford (Wüthrich, 1998) and have since been published (Pervushin et al., 1998b). In the case of ^{15}N-^{1}HN correlation spectroscopy the experiment transfers one of the two possible ^{15}N components of magnetization to ^{1}HN for detection, while the transfer of the second component is eliminated by phase cycling. In what follows we denote this magnetization transfer by the following, $N_{TR}(1-2I_z) \longrightarrow I_{TR}(1+2N_z)$, where O_i is the i component of O (N =^{15}N, I =^{1}HN) magnetization and TR indicates transverse magnetization. In 2D ^{15}N-^{1}HN correlation experiments a crosspeak at ($\omega_N - \pi J_{NH}$, $\omega_H + \pi J_{NH}$) results, where ω_N and ω_H are the Larmor frequencies of the ^{15}N and ^{1}HN spins, respectively, and J_{NH} ($J_{NH} < 0$) is the one bond ^{15}N-^{1}HN coupling constant. The multiplet component derived from this transfer relaxes slowly since contributions from dipolar and CSA interactions cancel, at least partially (Pervushin et al., 1997). It is particularly noteworthy that although only 1 of 4 frequency components is selected using this approach, a full 50% of the magnetization is, nevertheless, transferred by this procedure in the absence of relaxation. The component derived from the second pathway, $N_{TR}(1+2I_z) \longrightarrow I_{TR}(1-2N_z)$, which relaxes very efficiently and would normally give rise to a crosspeak at ($\omega_N + \pi J_{NH}$, $\omega_H - \pi J_{NH}$), is eliminated by a two-step phase cycle. Because only the narrow component of magnetization is selected, gains in resolution and sensitivity (evaluated by peak height) are obtained over conventional experiments in which the multiplet components are mixed through the application of individual pulses or decoupling elements during the sequence (see below).

In the case of a simple 2D ^{15}N-^{1}HN correlation experiment, elimination of this second pathway using the scheme proposed by Pervushin et al. (1997) is crucial, since a doubling of the number of resonances would otherwise result. However, in the case of triple resonance applications of the HNC variety, illustrated by the transfer scheme

$$^{1}\mathrm{HN} \xrightarrow{\tau_a} {}^{15}\mathrm{N} \xrightarrow{\tau_b} {}^{13}\mathrm{C} \xrightarrow{\tau_b} {}^{15}\mathrm{N} \xrightarrow{\tau_a} {}^{1}\mathrm{HN} \longrightarrow \mathrm{Acquire}, \quad (2)$$

where ^{15}N magnetization is in the transverse plane for extensive periods of time, active elimination of the $N_{TR}(1+2I_z) \longrightarrow I_{TR}(1-2N_z)$ pathway may not be necessary. This is because the component derived from this transfer relaxes extremely efficiently during the constant time periods ($2\tau_b \approx 2 \times 25$ ms, see below) in the experiment and can have a much more significant ^{1}HN linewidth than the narrow component from the desired pathway. For example, calculations suggest that for a molecular correlation time of 15 ns a multiplet ratio (corresponding to components derived from $N_{TR}(1-2I_z) \longrightarrow I_{TR}(1+2N_z)$ and $N_{TR}(1+2I_z) \longrightarrow I_{TR}(1-2N_z)$ of 6.5/1, 9.5/1 and 20/1 would be obtained at 500, 600 and 800 MHz, respectively. For

molecules tumbling with a correlation time of 25 ns, ratios of 13.5/1 (500 MHz), 23/1 (600 MHz) and 64/1 (800 MHz) are calculated. The above results are based on ^{15}N and ^{1}HN chemical shift anisotropy values of -170 and -10 ppm, respectively (Tessari et al., 1997; Tjandra et al., 1996; Tjandra and Bax, 1997), angles of 18° and 0° between the (assumed axially symmetric) principal components of the ^{15}N and ^{1}HN chemical shift tensors and the ^{15}N-^{1}HN bond (Tjandra et al., 1996), an ^{15}N-^{1}HN bond length of 1.02 Å and an S^2 value of 0.85. In addition a contribution of $0.52 \times \tau_C \times 10^9$ s^{-1} to the relaxation rates of the ^{1}HN multiplet components from the surrounding protons was employed, where τ_C is the overall correlation time (in ns), as established from experiments recorded on a sample of a methyl-protonated, highly deuterated maltose binding protein, protonated β-cyclodextrin complex (see below). Figure 1 illustrates the calculated multiplet ratio as a function of overall molecular correlation time for spectra recorded at 500–800 MHz. For more completely deuterated systems still larger ratios will be obtained. It is noteworthy that the above calculation assumes that magnetization derives exclusively from ^{1}HN at the start of the experiment. As described by Pervushin and coworkers (1998a), when components from both ^{1}HN and the directly attached heteroatom contribute to the signal further increases in the ratios presented above result.

The tolerable level of multiplet component suppression may vary depending on the application and the protein. Figure 1 suggests that for proteins with correlation times in excess of approximately 25 ns and for fields of 600 MHz or greater, active suppression of the $N_{TR}(1+2I_z) \longrightarrow I_{TR}(1-2N_z)$ pathway may not be necessary in many triple resonance applications. On the basis of this result we searched for TROSY-based schemes which would transfer either pathways, $N_{TR}(1\pm2I_z) \longrightarrow I_{TR}(1\mp2N_z)$, and which would be less sensitive to relaxation losses during such transfer than the schemes which have been proposed to date. This is a particularly important concern for macromolecular applications, even in the limit of highly deuterated molecules, since as we show below transverse relaxation times of proteins with τ_c values $\geq\approx$ 25 ns can be very short.

Figure 2 illustrates a set of pulse sequences that have been compared for spectral sensitivity and resolution. Although the experiments are of the HNCO variety (Kay et al., 1990), the conclusions obtained are equally valid for any class of triple resonance experiment in which ^{15}N magnetization resides in

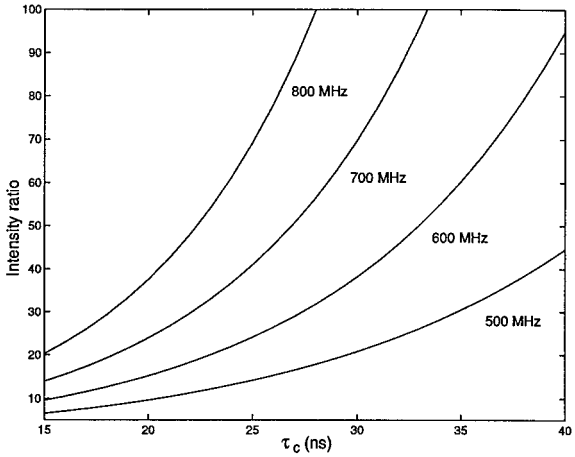

Figure 1. Intensity ratio (A/B) of components derived from the transfers $N_{TR}(1 - 2I_z)$ – A $\longrightarrow$ $I_{TR}(1+2N_z)$ and $N_{TR}(1+2I_z)$ – B $\longrightarrow$ $I_{TR}(1-2N_z)$ in HNC based triple resonance pulse schemes (see Equation 2), as a function of overall correlation time, τ_C. A value of $\tau_b = 25$ ms (see Equation 2) was employed, with ^{15}N and ^{1}HN chemical shift anisotropy values of -170 and -10 ppm, respectively, angles of 18° and 0° between the principal components of the ^{15}N and ^{1}HN chemical shift tensors, a ^{15}N-^{1}HN bond length of 1.02 Å and an S^2 value of 0.85. A ^{1}HN spin flip rate of $0.52 \times \tau_C \times 10^9 s^{-1}$ was employed (see text).

the transverse plane for a duration similar to that in the HNCO. In Figure 2a an HNCO-scheme which employs the TROSY principle and which eliminates the $N_{TR}(1+2I_z) \longrightarrow I_{TR}(1-2N_z)$ transfer pathway is shown. This sequence is based on the ^{15}N-^{1}HN HSQC discussed by Pervushin and coworkers previously (1997), except that magnetization originating on both ^{15}N and ^{1}HN is selected and both cosine and sine-modulated ^{15}N t_2-components are returned for observation, as described recently by Wüthrich (1998) and by Pervushin et al. (1998b). Note that it is essential that the ^{1}H spin state not be inverted during the interval extending between points a and b in the sequence so that cross-correlation between ^{15}N-^{1}HN dipolar and ^{15}N CSA interactions is operative during the complete interval. This is necessary for all of the experiments illustrated in the Figure. In Figure 2b an HNCO scheme in which ^{15}N magnetization is transferred back to ^{1}HN for detection using the enhanced sensitivity (Palmer et al., 1991) gradient selection approach (Kay et al., 1992; Schleucher et al., 1993) is illustrated. Note that this sequence transfers both of the pathways, $N_{TR}(1\pm2I_z) \longrightarrow I_{TR}(1\mp2N_z)$, with elimination of the unwanted multiplet component derived from $N_{TR}(1+2I_z) \longrightarrow I_{TR}(1-2N_z)$ achieved passively through attenuation by relaxation during the pulse scheme. As described in detail below, relaxation

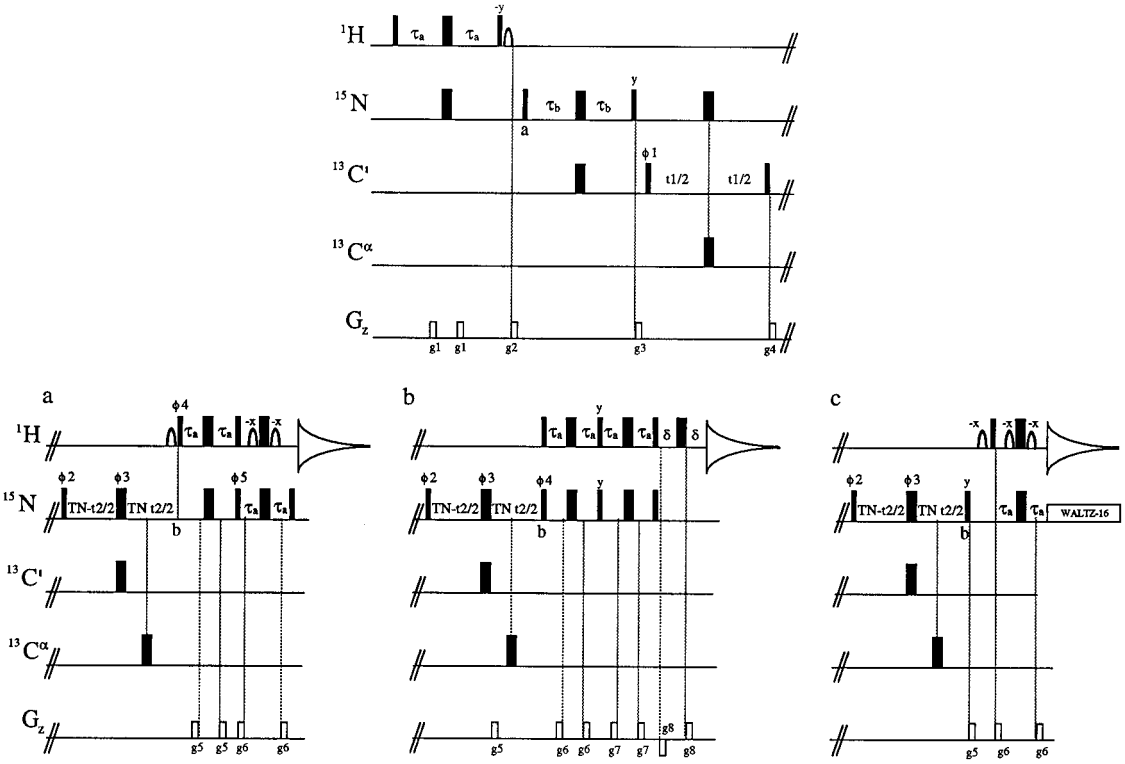

Figure 2. (a) TROSY-HNCO using the scheme of Pervushin and coworkers (1997) with modifications to ensure that both cosine and sine modulated ^{15}N magnetization components are observed (Wüthrich, 1998; Pervushin et al., 1998b). (b) TROSY-HNCO modified using the gradient enhanced sensitivity coherence transfer scheme (Kay et al., 1992; Schleucher et al., 1993) for transfer of magnetization from ^{15}N to ^{1}HN prior to detection. Schemes (a) and (b) employ the TROSY principle during evolution of both ^{15}N and ^{1}HN magnetization. (c) TROSY-HNCO with the TROSY principle applied only for ^{15}N magnetization. Note that magnetization originating on both ^{15}N and ^{1}HN spins is transferred to observable signal in all three schemes, as described by Pervushin et al. (1998a). Depending on the spectrometer it may be necessary to change the phase of the nonselective ^{1}H pulse prior to gradient g2 from $-$y to y in order to add constructively the ^{15}N-originating component with the ^{1}HN-originating component. To establish whether the phase is correct the sensitivity of 1D traces can be compared with the phase set to $-$y and y; the correct setting of the phase produces more signal. All phase settings have been verified on Varian Unity+ and Inova spectrometers. All narrow (wide) pulses are applied with a flip angle of 90° (180°). ^{1}H, ^{15}N and ^{13}C carriers are positioned at the water line, 119 and 176 ppm, respectively. All ^{1}H rectangular pulses are applied with a 31 kHz field, while ^{15}N and carbonyl (^{13}C′) pulses employ fields of 5.5 and $\Delta/\sqrt{15}$ kHz, respectively, where Δ is the difference in Hz between the centers of the ^{13}C$^{\alpha}$ and ^{13}C′ chemical shift regions (Kay et al., 1990). ^{13}C$^{\alpha}$ pulses are phase modulated (118 ppm) (Boyd and Scoffe, 1989; Patt, 1992) and are applied with a field of $\Delta/\sqrt{3}$ kHz. Water selective pulses, denoted by the shaped ^{1}H pulses, are of duration 2 ms with the phase of each pulse adjusted to minimize residual water during acquisition. In the case of sequence (c), ^{15}N decoupling during acquisition employs a 1 kHz field. The delays used are: $\tau_a = 2.3$ ms, $\tau_b = 12.4$ ms, $\delta = 0.25$ ms and $T_N = 12.4$ ms. Sequence (a): The phase cycle employed is: $\phi1 = 2(x),2(-x)$; $\phi2 = 4(x),4(y)$; $\phi3 = (x,-x)$; $\phi4 = -y$; $\phi5 = -y$; receiver $= 2(y),2(-y),2(-x),2(x)$. In order to ensure that the slowest relaxing component is selected it is best to compare a 2D (^{15}N-^{1}HN) spectrum recorded with scheme (a) with a regular 2D ^{15}N-^{1}HN correlation spectrum recorded without ^{1}H decoupling in t_1 or ^{15}N decoupling during acquisition. The peak of interest in scheme (a) corresponds to the most downfield (upfield) F_1 (F_2) component in the undecoupled spectrum. If the 'wrong' component is selected in sequence (a), change the receiver phase to $2(y),2(-y),2(x),2(-x)$. Note that the signal from the 'wrong' component will be noticeably smaller than from the correct component. Quadrature in F_1 is achieved by States-TPPI (Marion et al., 1989) of $\phi1$, while quadrature in F_2 is achieved by incrementing the phases of $\phi4$, $\phi5$ and the receiver by 180°, with the phase $\phi2$ changed to $4(x),4(-y)$ and by recording a separate data set with these phases for each t_2 value. Data sets are subsequently combined using the same procedure as for the gradient enhanced sensitivity method. The phase $\phi2$ and the phase of the receiver are incremented by 180° for each successive complex t_2 point (Marion et al., 1989). The duration and strengths of the gradients are: g1 = (0.5 ms, 5 G/cm); g2 = (1 ms, 15 G/cm); g3 = (0.75 ms, 10 G/cm); g4 = (0.5 ms, 10 G/cm); g5 = (0.4 ms, 3.1 G/cm); g6 = (0.2 ms, 4.95 G/cm). Sequence (b): The phase cycle for sequence (b) is: $\phi1 = 2(x),2(-x)$; $\phi2 = (y,-y)$; $\phi3 = 4(x),4(-x)$; $\phi4 = x$; receiver $= x,2(-x),x$. Quadrature in F_1 is achieved by States-TPPI of $\phi1$, while F_2 quadrature is achieved by the enhanced sensitivity pulsed field gradient method, where for each value of t_2 separate data sets are recorded for ($g5,\phi4$) and ($-g5,\phi4 + 180°$). For each successive t_2 value, $\phi2$ is incremented by 180° along with the phase of the receiver. The duration and strengths of the gradients are: g1 = (0.5 ms, 5 G/cm); g2 = (1 ms, 15 G/cm); g3 = (0.75 ms, 10 G/cm); g4 = (0.5 ms, 10 G/cm); g5 = (1.25 ms, 30 G/cm); g6 = (0.4 ms, 2.9 G/cm); g7 = (0.4 ms, 5.35 G/cm); g8 = (62.5 μs, 28.75 G/cm). Sequence (c): The phase cycle is: $\phi1 = 2(x),2(-x)$; $\phi2 = (x,-x)$; $\phi3 = 4(x),4(-x)$; receiver $= x,2(-x),x$. Quadrature in F_1 and F_2 is achieved by States-TPPI of $\phi1$ and $\phi2$, respectively. The duration and strengths of the gradients are: g1 = (0.5 ms, 5 G/cm); g2 = (1 ms, 15 G/cm); g3 = (0.75 ms, 10 G/cm); g4 = (0.5 ms, 10 G/cm); g5 = (1 ms, 10 G/cm); g6 = (0.2 ms, 4.5 G/cm).

losses during the final part of this sequence are less than in the experiment of Figure 2a. Finally, a pulse sequence is presented in Figure 2c where ^{15}N magnetization is transferred equally to the two ^{1}H multiplet components and ^{15}N decoupling applied during detection. Unlike the schemes of Figures 2a and 2b, where the TROSY principle is applied for both ^{15}N and ^{1}HN magnetization, in the sequence of Figure 2c the use of TROSY is limited to the interval in which ^{15}N magnetization is present.

The differences in relaxation losses that occur in the schemes of Figure 2a and 2b can be appreciated by the following qualitative argument. Using the first line of the phase cycle for each sequence described in the legend to Figure 2, focusing only on the $N_{TR}(1-2I_z) \longrightarrow I_{TR}(1+2N_z)$ transfer and neglecting all multiplicative factors, the magnetization at point b is given by

$$N_x(1-2I_z)\cos\{(\omega_N-\pi J_{NH})t_1\}+ N_y(1-2I_z)\sin\{(\omega_N-\pi J_{NH})t_1\} \quad (3.1)$$

and

$$N_y(1-2I_z)\cos\{(\omega_N-\pi J_{NH})t_1+\phi\}- N_x(1-2I_z)\sin\{(\omega_N-\pi J_{NH})t_1+\phi\}, \quad (3.2)$$

for sequences 2a and 2b, respectively. In Equation 3.2 ϕ is the phase generated by application of coherence transfer gradient g5 and will vary linearly with position of the spin in the field. Considering only the $N_y(1-2I_z)$ terms, the scheme extending from point b in Figure 2a transfers the N_y component to I_x according to

$$N_y \xrightarrow{90_{\phi4}} N_y \xrightarrow{2\tau_a} 2N_xI_z \underset{90_{\phi5(N)}}{\overset{90_{x(I)}}{\longrightarrow}} 2N_zI_y \xrightarrow{2\tau_a} I_x \underset{90_{x(N)}}{\longrightarrow} I_x \quad (4.1)$$

and the $2N_yI_z$ term to $2N_zI_x$ according to

$$2N_yI_z \xrightarrow{90_{\phi4(I)}} 2N_yI_x \xrightarrow{2\tau_a} 2N_yI_x \underset{90_{\phi5(N)}}{\overset{90_{x(I)}}{\longrightarrow}} 2N_yI_x \xrightarrow{2\tau_a} 2N_yI_x \underset{90_{x(N)}}{\longrightarrow} 2N_zI_x, \quad (4.2)$$

where all multiplicative factors are again omitted. Thus, during the transfer indicated in Equation 4.1 magnetization relaxes during the first and second $2\tau_a$ periods with time constants given by $T_{2,N}$ and by $T_{2,H}$, respectively, where $T_{2,N}$ and $T_{2,H}$ are ^{15}N and ^{1}HN transverse relaxation times. In contrast during the transfer described by Equation 4.2 ^{15}N-^{1}HN double- and zero-quantum coherences are present for the complete transfer duration ($4\tau_a$). This situation is contrasted with the scheme of Figure 2b, where starting from the $N_y(1\text{-}2I_z)$ component at point b in the sequence the following magnetization transfers are obtained,

$$N_y \underset{90_{\phi4(N)}}{\overset{90_{x(I)}}{\longrightarrow}} N_z \xrightarrow{2\tau_a} N_z \underset{90_{y(N)}}{\overset{90_{y(I)}}{\longrightarrow}} N_x \xrightarrow{2\tau_a} 2N_yI_z \underset{90_{x(N)}}{\overset{90_{x(I)}}{\longrightarrow}} 2N_zI_y \quad (5.1)$$

and

$$2N_yI_z \underset{90_{\phi4(N)}}{\overset{90_{x(I)}}{\longrightarrow}} 2N_zI_y \xrightarrow{2\tau_a} I_x \underset{90_{y(N)}}{\overset{90_{y(I)}}{\longrightarrow}} I_z \xrightarrow{2\tau_a} I_z \underset{90_{x(N)}}{\overset{90_{x(I)}}{\longrightarrow}} I_y. \quad (5.2)$$

Note that in both cases (Equations 5.1 and 5.2) magnetization resides along the z-axis for one of the $2\tau_a$ periods and hence the relaxation losses are reduced.

A more quantitative evaluation of the effects of relaxation during each of the $N_{TR}(1-2I_z) \longrightarrow I_{TR}(1+2N_z)$ transfers occurring in sequences 2a and 2b must consider how relaxation influences both $N_x(1-2I_z)$ and $N_y(1-2I_z)$ components of magnetization. It can be shown that relaxation attenuates the signal of interest by the factors

$$0.25\{\exp(-2\tau_a/T_{2,MQ})+\exp(-2\tau_a/T_{2,N})\}\{\exp(-2\tau_a/T_{2,MQ})+\exp(-2\tau_a/T_{2,H})\} \quad (6.1)$$

and

$$0.25\{\exp(-2\tau_a/T_{2,MQ})+1\}\{\exp(-2\tau_a/T_{2N}) + \exp(-2\tau_a/T_{2,H})\}\exp(-2\delta/T_{2,H}) \quad (6.2)$$

for sequences 2a and 2b, respectively, where $T_{2,MQ}$ is the relaxation time for ^{15}N-^{1}HN double/zero quantum coherences. In Equations 6.1 and 6.2 signal decay from the relaxation of longitudinal magnetization has been neglected since $T_{1,N}$, $T_{1,H} \gg 2\tau_a$, double and zero quantum coherences are assumed to relax at the same rate and the value of τ_a is chosen such that $\sin(2\pi J_{NH}\tau_a) \approx 1$.

The pulse schemes of Figure 2 were evaluated by calculating the signal to noise ratios in spectra generated from each of the sequences, as described in Materials and methods. The complex of MBP (370 residues) and β-cyclodextrin used in the present analysis has a molecular weight of 42 kDa, with correlation times of 23 ± 0.8 and 46 ± 2 ns at 25 and 5 °C, respectively, as established by ^{15}N spin relaxation experiments (Farrow et al., 1994). Values of $T_{2,N}$, $T_{2,H}$ and $T_{2,MQ}$ were measured at both temperatures for 91 well resolved residues in MBP and ($T_{2,N}$, $T_{2,H}$, $T_{2,MQ}$) = (32.7 (3.8) ± 0.6 ms, 17.5 (3.0) ± 0.7 ms, 22.5 (4.7) ± 0.4 ms), ($T_{2,N}$, $T_{2,H}$, $T_{2,MQ}$) = (16.4 (1.9) ± 1.0 ms, 9.7 (1.5) ± 0.7 ms, 12.7 (2.3) ± 0.5 ms) obtained at 25 and 5 °C, respectively. (Note that a value of 32.7 (3.8) ± 0.6 ms corresponds to an average relaxation time of 32.7 ms, with a standard deviation of 3.8 ms for the 91 peaks and an error of 0.6 ms.) On the basis of the measured relaxation times, Equations 6.1, 6.2 and delays indicated in the legend to Figure 2, MBP spectra recorded at 25 °C with sequence 2b are predicted to be a factor of 1.08 more sensitive than spectra obtained with scheme 2a, while a gain of a factor of 1.16 is calculated for spectra recorded at 5 °C. The gains of 1.12 ± 0.03 (25 °C) and 1.19 ± 0.07 (5 °C) observed experimentally for sequence 2b relative to 2a agree reasonably well with the values of 1.08 and 1.16 calculated. It is noteworthy that gains of a factor of 1.46 ± 0.10 and 1.53 ± 0.18 are measured for sequence 2b relative to 2c from spectra recorded at 25 and 5 °C, respectively. Figures 3a, b, c illustrate F_2 slices from 2D (F_2-F_3) HNCO spectra of MBP at 5 °C obtained with sequences b, a and c of Figure 2, respectively. Figure 3d shows the intensity ratios of crosspeaks from 3D spectra recorded at 5 °C using sequences a and b of Figure 2. All of the 270 crosspeaks examined were more intense in spectra recorded with scheme 2b relative to sequence 2a.

As a matter of interest we have also compared S/N ratios in spectra obtained with the sequences of Figure 2 with a spectrum recorded using an HNCO pulse sequence that we published several years ago where ^{1}H decoupling was employed during the evolution of ^{15}N magnetization and ^{15}N decoupling used during acquisition (Kay et al., 1994). The relative S/N in HNCO spectra of MBP recorded at 25 °C is reduced in the non-TROSY based sequence by a factor of 2.4 relative to the scheme of Figure 2b. It is clear that significant benefits are achieved using the TROSY principle.

Relaxation during the $N_{TR}(1-2I_z) \longrightarrow I_{TR}(1+2N_z)$ transfers in both of the sequences of Figures 2a and 2b is important for reasons other than optimization of S/N in the experiments. As discussed above in the context of the transfer of $N_{TR}(1-2I_z)$ to $I_{TR}(1+2N_z)$ (see Equations 4 and 5), the N_{TR} and the $2N_{TR}I_z$ components relax differently because of the different pathways that each element takes during the sequence of pulses and delays that relays magnetization from ^{15}N to ^{1}HN. It is straightforward to show that this differential relaxation results in the creation of a small amount of ^{1}HN signal of the form $I_{TR}(1-2N_z)$, in addition to the expected $I_{TR}(1+2N_z)$. Thus, doublet components are observed in the acquisition dimen-

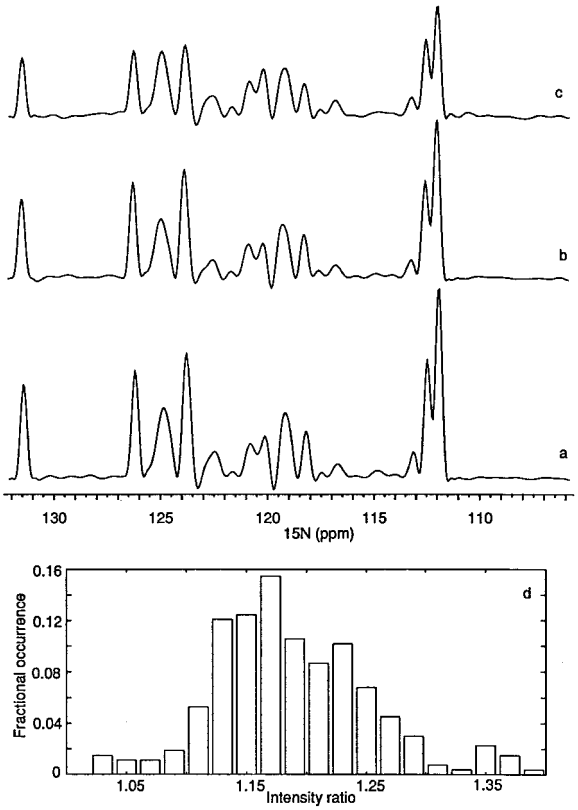

Figure 3. F_2 traces from 2D HNCO (F_2-F_3) spectra recorded of the methyl protonated, highly deuterated MBP/β-cyclodextrin complex (Gardner and Kay, 1997) at 5 °C using the pulse sequences illustrated in Figure 2. (a) Trace from the data set recorded with the sequence of Figure 2b. (b) Trace from the spectrum recorded with the scheme of Figure 2a. (c) Trace from the data set obtained with sequence 2c. Note that F_3 chemical shifts are displaced upfield by an amount of $|J_{NH}|/2$ Hz in spectra recorded with schemes 2a and 2b relative to sequence 2c. Trace c is at 8.9 ppm in F_3. (d) Relative S/N in spectra recorded with the sequences of Figure 2a and b. The intensity ratio is defined by Equation 1. Crosspeaks in the spectrum recorded with the sequence of Figure 2b are more intense by approximately 20% than crosspeaks from the data set obtained with the scheme of Figure 2a (5 °C).

sion, separated by J_{NH}. Neglecting the differential relaxation of the two doublet components during acquisition, the relative peak heights of the two doublet components are given by

$$\{\exp(-2\tau_a/T_{2,H})\exp(2\tau_a/T_{2,MQ}) + 1\}/ \{\exp(-2\tau_a/T_{2,H})\exp(2\tau_a/T_{2,MQ}) - 1\} \quad (7.1)$$

$$\{\exp(-2\tau_a/T_{2,H})\exp(2\tau_a/T_{2,N}) + 1\}/ \{\exp(-2\tau_a/T_{2,H})\exp(2\tau_a/T_{2,N}) - 1\} \quad (7.2)$$

for the sequences of Figure 2a and 2b, respectively. Using the relaxation parameters measured for MBP at 25 °C the minor doublet component is calculated to be approximately 3% and 6% of the major component for sequences 2a and 2b. These values are larger than observed experimentally (2% and 4% for experiments of Figure 2a and 2b) due to the additional attenuation from relaxation that occurs during acquisition with $I_{TR}(1-2N_z)$ relaxing more rapidly than $I_{TR}(1+2N_z)$.

In summary, a scheme for the improvement in the sensitivity of HNC-type triple resonance TROSY-based pulse schemes is described, based on the minimization of relaxation losses that occur during transfer of magnetization from ^{15}N to ^{1}HN prior to signal detection. Suppression of the rapidly relaxing component of magnetization is achieved by relaxation that occurs during the pulse sequence. The method presented is thus well suited for triple resonance applications on high molecular weight proteins ($\tau_C > 20$ ns) recorded at high magnetic fields where the undesired pathway is severely attenuated by relaxation.

Acknowledgements

The authors thank Mr Randall Willis (Hospital for Sick Children) and Dr. Kevin Gardner (University of Toronto) for preparation of the MBP sample used in the present study. This research was supported by the Medical Research Council of Canada. L.E.K. is an International Howard Hughes Research Scholar.

Note added in proof

In cases where the unwanted component arising from the $N_{TR}(1 + 2I_z) \longrightarrow I_{TR}(1 - 2N_z)$ transfer does not decay to acceptable levels during the course of the delays in the pulse scheme, it is still possible to use the sequence of Figure 2b with improved sensitivity relative to other implementations of TROSY (i.e., Figure 2a). In this case this component must be actively suppressed. This is readily accomplished by changing the phase of the ^{15}N pulse at point a in the sequence of Figure 2 to 45° (or −45°, depending on the spectrometer; the correct phase is the one which gives the most signal!), by changing the phase of the 90° ^{1}H pulse prior to the water selective pulse (from −y to y), by adding a ^{1}H 180° pulse (composite) at a delay of $1/(8J_{NH})$ from point a in the sequence and by inverting the phase of the water selective pulse immediately before gradient g2. Experiments on MBP at 37 °C ($\tau_C \approx 17$ ns) and 25 °C ($\tau_C \approx 23$ ns) where the unwanted transfer is actively eliminated indicate sensitivity gains of a few percent over the scheme of Figure 2a. This will be described in more detail elsewhere.

References

Bax, A. (1994) *Curr. Opin. Struct. Biol.*, **4**, 738–744.
Boyd, J. and Scoffe, N. (1989) *J. Magn. Reson.*, **85**, 406–413.
Delaglio, F., Grzesiek, S., Vuister, G.W., Zhu, G., Pfeifer, J. and Bax, A. (1995) *J. Biomol. NMR*, **6**, 277–293.
Farmer, B.T., Constantine, K.L., Goldfarb, V., Friedrichs, M.S., Wittekind, M., Yanchunas, J., Robertson, J.G. and Mueller, L. (1996) *Nat. Struct. Biol.*, **3**, 995–997.
Farrow, N.A., Muhandiram, R., Singer, A.U., Pascal, S.M., Kay, C.M., Gish, G., Shoelson, S.E., Pawson, T., Forman-Kay, J.D. and Kay, L.E. (1994) *Biochemistry*, **33**, 5984–6003.
Gardner, K.H. and Kay, L.E. (1997) *J. Am. Chem. Soc.*, **119**, 7599–7600.
Gardner, K.H., Zhang, X., Gehring, K. and Kay, L.E. (1998) *J. Am. Chem. Soc.*, **120**, 11738–11748.
Garrett, D.S., Powers, R., Gronenborn, A.M. and Clore, G.M. (1991) *J. Magn. Reson.*, **95**, 214–220.
Garrett, D.S., Seok, Y.J., Liao, D.I., Peterkofsky, A., Gronenborn, A.M. and Clore, G.M. (1997) *Biochemistry*, **36**, 2517–2530.
Kay, L.E. and Gardner, K.H. (1997) *Curr. Opin. Struct. Biol.*, **7**, 722–731.
Kay, L.E., Ikura, M., Tschudin, R. and Bax, A. (1990) *J. Magn. Reson.*, **89**, 496–514.
Kay, L.E., Keifer, P. and Saarinen, T. (1992) *J. Am. Chem. Soc.*, **114**, 10663–10665.
Kay, L.E., Xu, G.Y. and Yamazaki, T. (1994) *J. Magn. Reson.*, **A109**, 129–133.
Marion, D., Ikura, M., Tschudin, R. and Bax, A. (1989) *J. Magn. Reson.*, **85**, 393–399.
Palmer, A.G., Cavanagh, J., Wright, P.E. and Rance, M. (1991) *J. Magn. Reson.*, **93**, 151–170.
Patt, S.L. (1992) *J. Magn. Reson.*, **96**, 94–102.
Pervushin, K., Riek, R., Wider, G. and Wüthrich, K. (1997) *Proc. Natl. Acad. Sci. USA*, **94**, 12366–12371.
Pervushin, K., Riek, R., Wider, G. and Wüthrich, K. (1998a) *J. Am. Chem. Soc.*, **120**, 6394–6400.

Pervushin, K., Wider, G. and Wüthrich, K. (1998b) *J. Biomol. NMR*, **12**, 345–348.
Schleucher, J., Sattler, M. and Griesinger, C. (1993) *Angew. Chem. Int. Ed. Engl.*, **32**, 1489–1491.
Shan, X., Gardner, K.H., Muhandiram, D.R., Rao, N.S., Arrowsmith, C.H. and Kay, L.E. (1996) *J. Am. Chem. Soc.*, **118**, 6570–6579.
Tessari, M., Vis, H., Boelens, R., Kaptein, R. and Vuister, G. (1997) *J. Am. Chem. Soc.*, **119**, 8985–8990.
Tjandra, N., Szabo, A. and Bax, A. (1996) *J. Am. Chem. Soc.*, **118**, 6986–6991.
Tjandra, N. and Bax, A. (1997) *J. Am. Chem. Soc.*, **119**, 8076–8082.
Venters, R.A., Farmer, B.T., Fierke, C.A. and Spicer, L.D. (1996) *J. Mol. Biol.*, **264**, 1101–1116.
Wüthrich, K. (1998) In *Third European Conference on Stable Isotope Aided NMR of Biomolecules* (Eds. Campbell, I., Laue, E. and Roberts, G.), St. John's College, Oxford.
Yu, L., Petros, A.M., Schnuchel, A., Zhong, P., Severin, J.M., Walter, K., Holzman, T.F. and Fesik, S.W. (1997) *Nat. Struct. Biol.*, **4**, 483–489.
Zhu, G. and Bax, A. (1990) *J. Magn. Reson.*, **90**, 405–410.